Supplementary Information

Bias-Free, High-Rate Solar Hydrogen Production in Alkaline Media with a NiCo-Coupled Perovskite Photocathode

Minseo Lee‡, Wooyeon Kim‡, Hayoung Kim‡, Seoyeong Lee, Min Jae Ko, and Youn Jeong Jang**

Department of Chemical Engineering, Hanyang University, 222, Wangsimni-ro, Seongdong-gu, Seoul, 04763, Republic of Korea

*Correspondence: mjko@hanyang.ac.kr (M. J. K.) and yjang53@hanyang.ac.kr (Y. J. J)

‡These authors contributed equally: Minseo Lee, Wooyeon Kim, Hayoung Kim

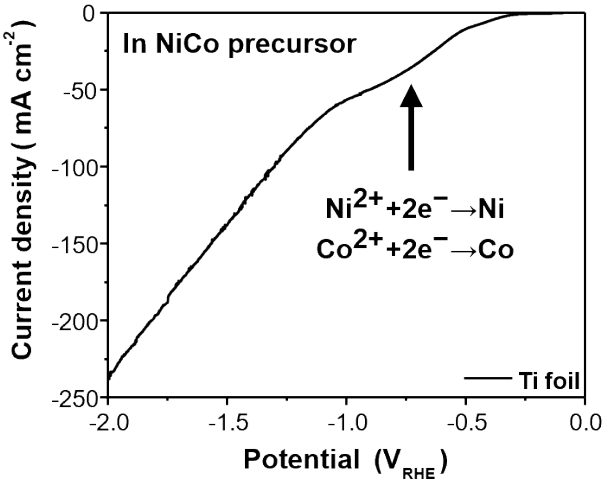

Fig. S1 Linear sweep voltammetry (LSV) curve of Ti foil in NiCo precursor.

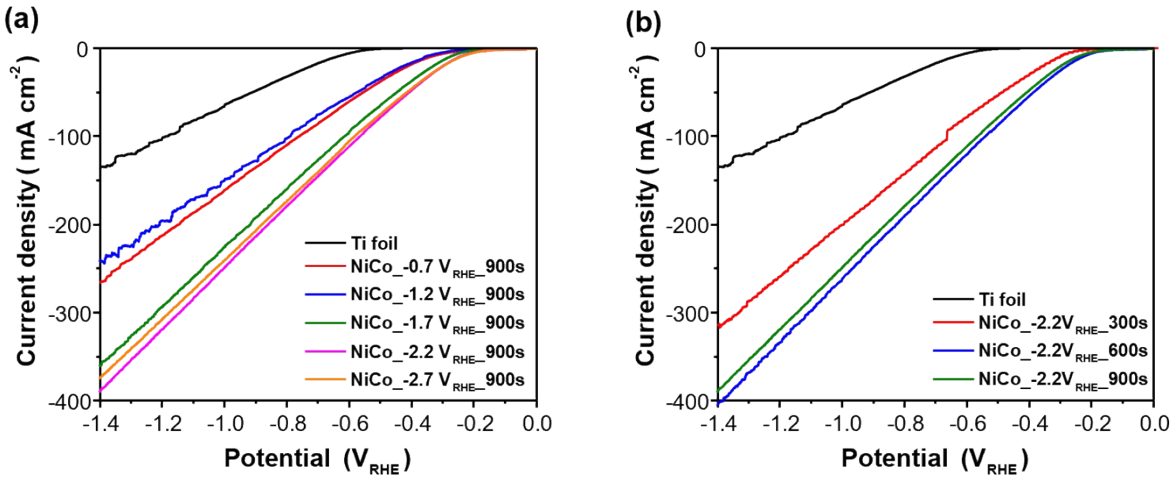

Fig. S2 LSV curves in 1M KOH depending on the deposition (a) potential and (b) time of NiCo catalyst for hydrogen evolution reaction (HER).

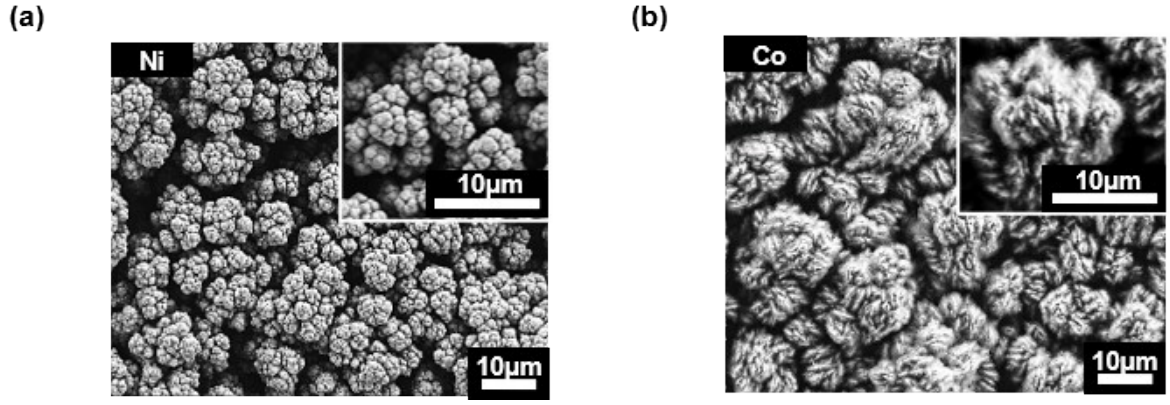

Fig. S3 Field-emission scanning electron microscopy (FE-SEM) images of (a) Ni and (b) Co. The inserts show higher-magnification images.

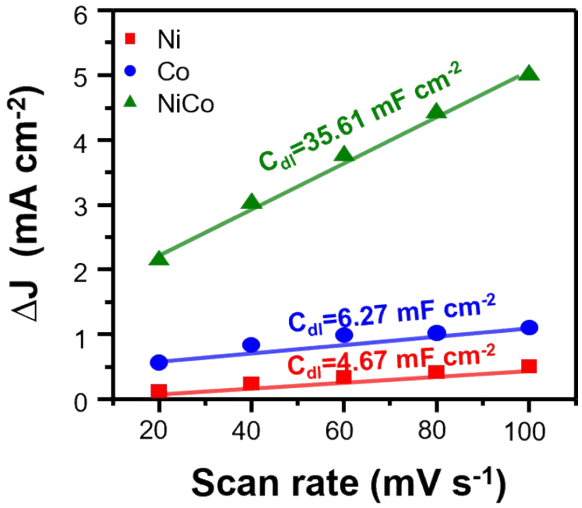

Fig. S4 Evaluation of **e**lectric double layer capacitance (C_{dl}) for Ni, Co and NiCo catalysts estimated from CV curves at scan rates of 20, 40, 60, 80, 100 mV s^{-1}.

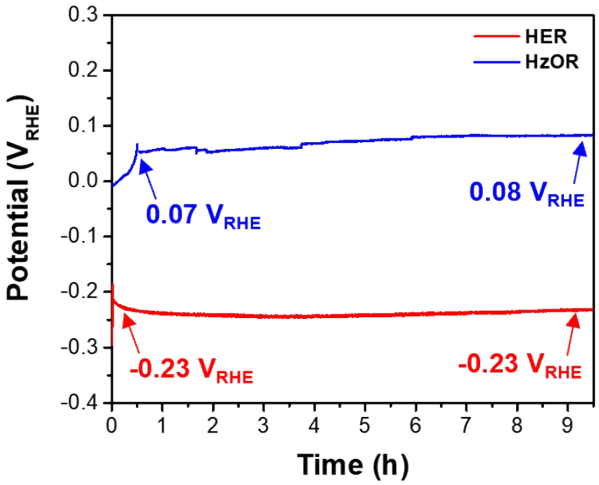

Fig. S5 Chronopotentiometry at 10 mA cm^{-2} of NiCo in 1 M KOH (red) and 1 M KOH + 0.5 M hydrazine (blue).

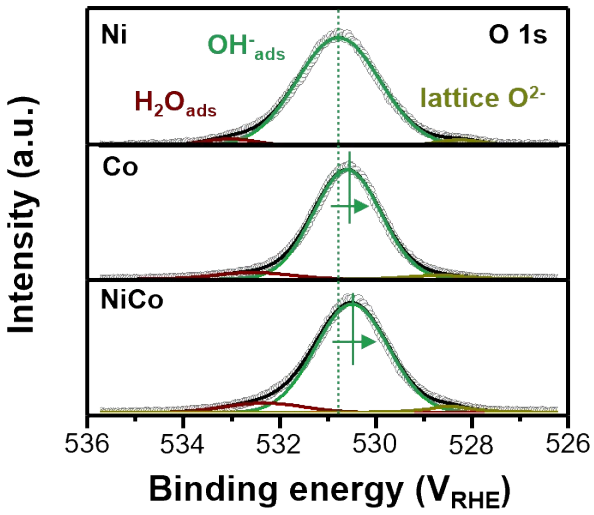

Fig. S6 X-ray photoelectron spectroscopy (XPS) spectra for O 1s of Ni, Co, and NiCo.

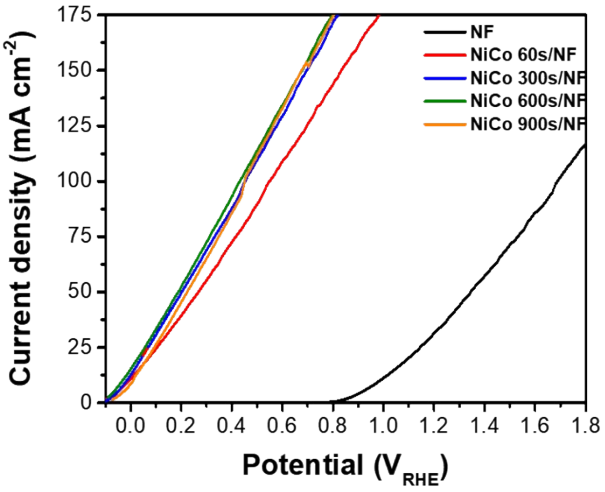

Fig. S7 LSV curves of Ni foam in 1 M KOH + 0.5 M hydrazine depending on the deposition time of NiCo catalyst for HzOR**.**

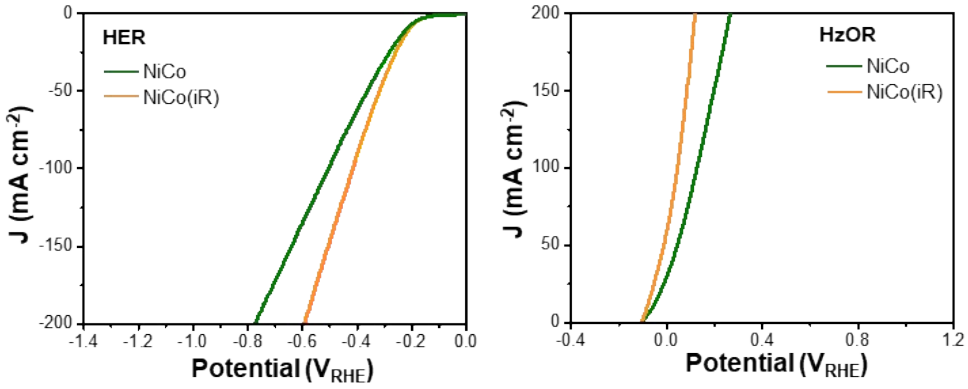

Fig. S8 LSV curves of the NiCo catalyst for HER and HzOR before and after iR correction.

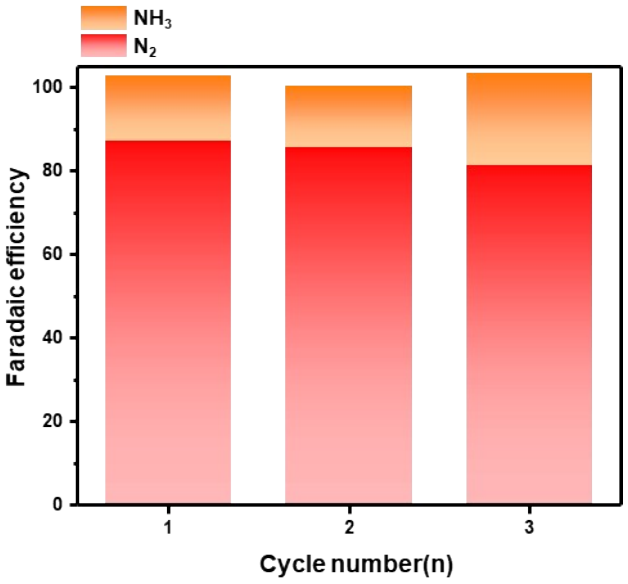

Fig. S9 Faradaic efficiency of NiCo/NF for HzOR over cycling

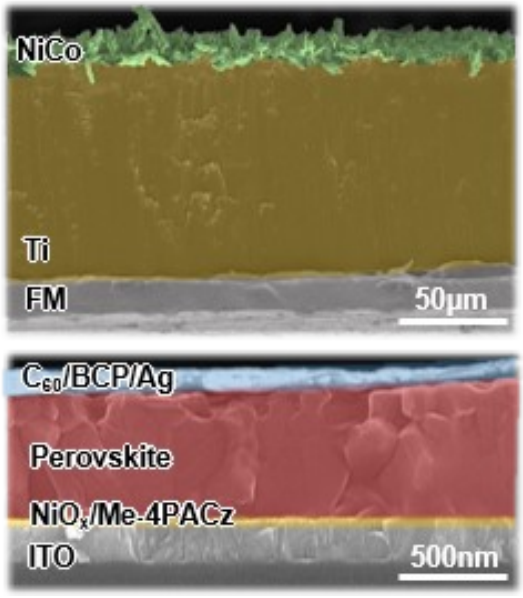

Fig. S10 Cross-sectional SEM image of the perovskite/NiCo photocathode.

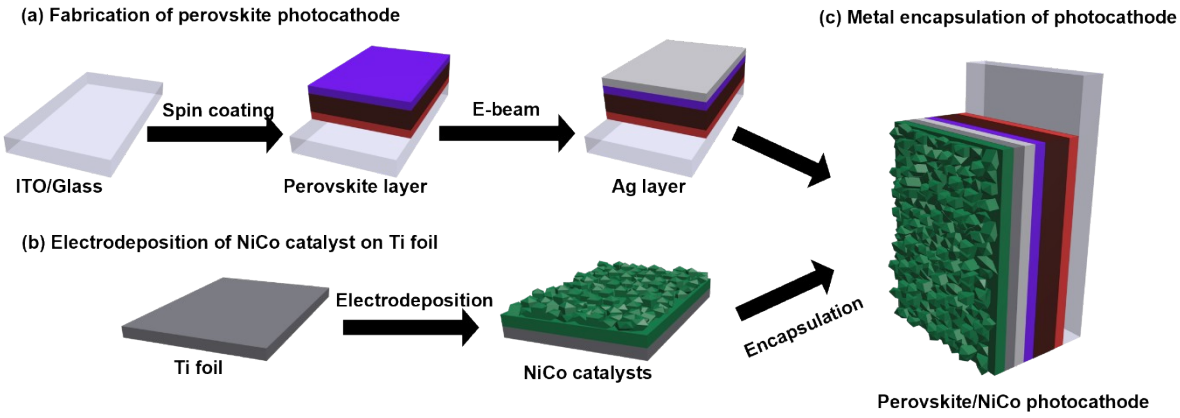

Fig. S11 Schematic illustration of the fabrication process for the perovskite photocathode and NiCo catalyst.

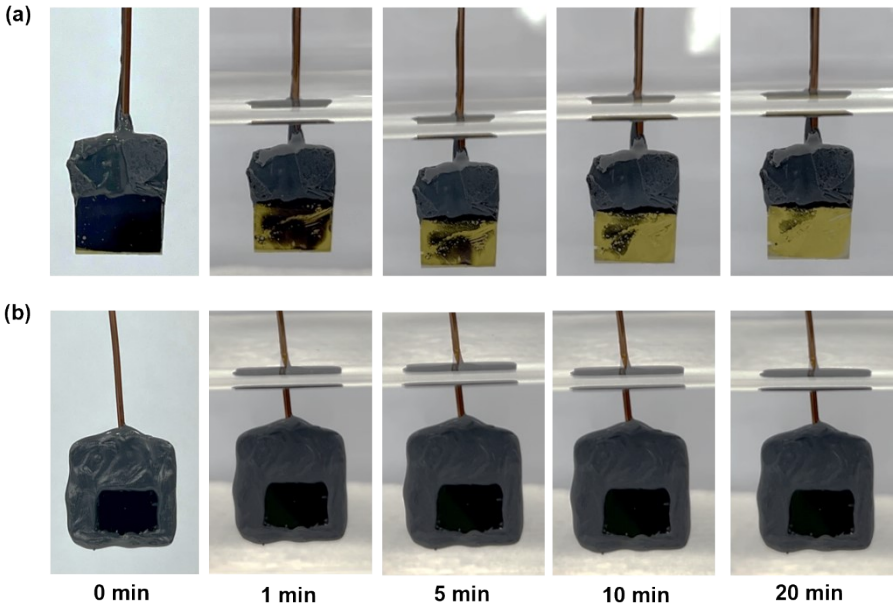

Fig. S12 Optical images of perovskite photocathode (a) without and (b) with encapsulation.

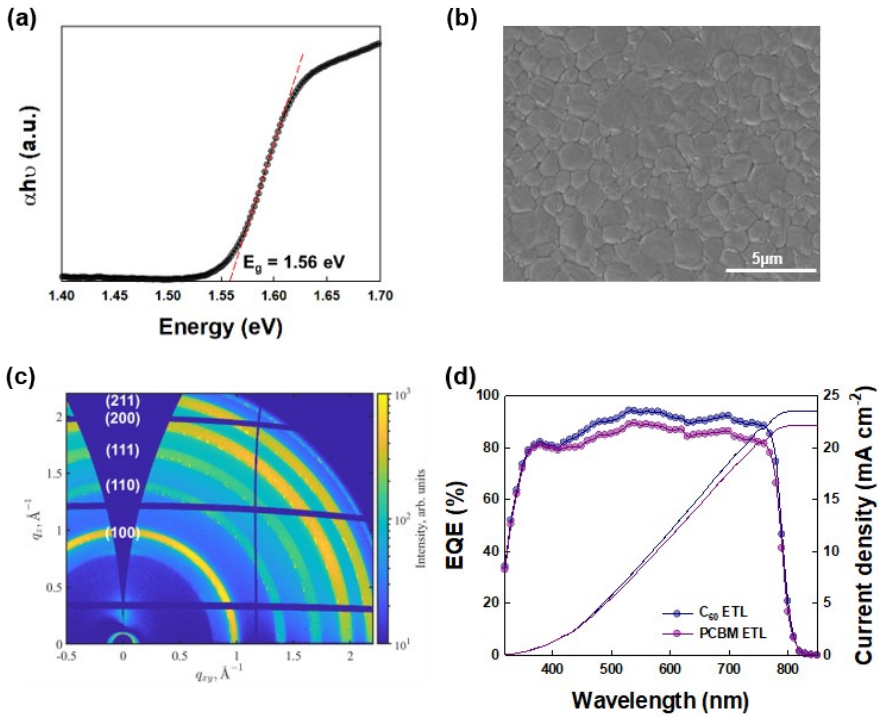

Fig. S13 (a) Tauc plots showing the optical bandgaps. (b) Top-view SEM image and (c) grazing incidence wide-angle X-ray scattering (GIWAXS) patterns of the perovskite film (d) External quantum efficiency (EQE) spectra of perovskite solar cells with different ETLs and integrated J_{SC} calculated from EQE.

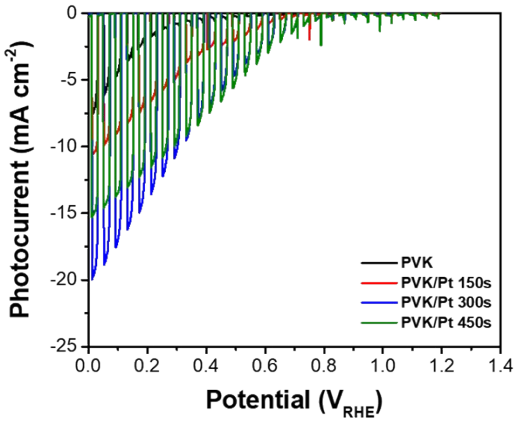

Fig. S14 LSV curves of lead halide perovskite (PVK) photocathode depending on the deposition time of Pt.

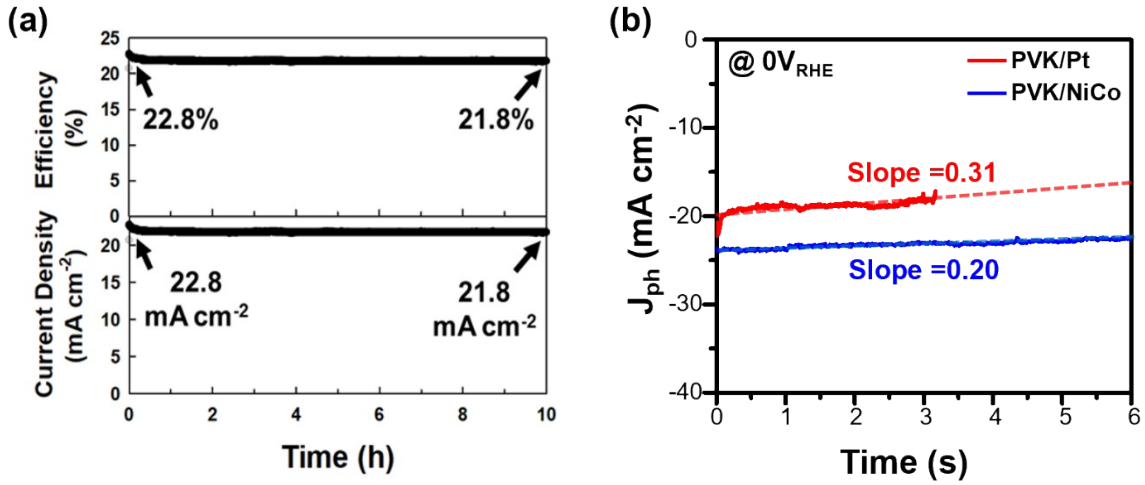

Fig. S15 (a) Operational stability test of perovskite solar cells under maximum power point tracking (MPPT) conditions under ambient conditions. (b) *J-t* curve at 0 V_{RHE} of PVK/Pt and PVK/NiCo photocathode for 6 h.

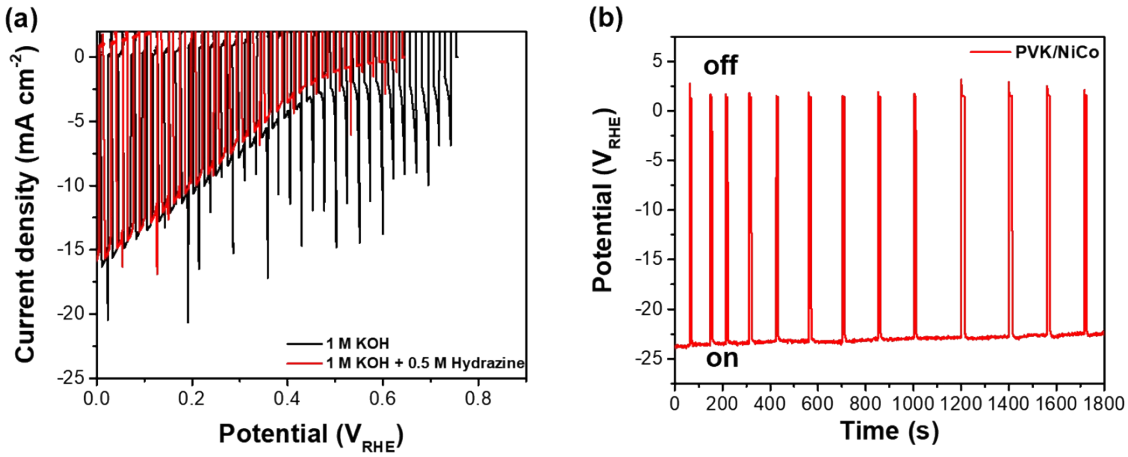

Fig. S16 (a) LSV curves depending on hydrazine and (b) chronoamperometry of PVK/NiCo photocathode in 1 M KOH + 0.5 M hydrazine.

Table S1 The composition of electrodeposited NiCo catalyst measured by inductively coupled plasma mass spectrometry (ICP-MS).

Method	Ni	Co	Ni/Co ratio
ICP-MS (total, mol)	1.28×10^{-4}	1.41×10^{-4}	0.91

Table S2 EIS fitting parameters for Ni, Co, and NiCo.

Catalyst	R_s (Ω)	R_{ct} (Ω)
Ni	3.22 ±0.29	2.29 ±0.18
Co	3.88 ±0.30	2.23 ±0.15
NiCo	3.53 ±0.18	1.59 ±0.11

Table S3 Faradaic efficiency distribution(%) of N_2 and NH_3 during HzOR.

Cycle number	N_2 (%)	NH_3 (%)
1	87.22	15.61
2	85.62	14.59
3	81.44	22.14

Table S4 The comparison of the overpotential at 10 mA cm^{-2} (η_{10}) for HzOR and HER.

Catalyst	HER η_{10} (mV)	HzOR η_{10} (mV)	Reference
Ni	218.4	285.2	This work
Co	286.8	274.6	This work
NiCo	191.2	267.9	This work
NiS_2/TiM	220	390	*1*
CoSe/CFP	204	321	*2*
Pd/$NiCo_2O_4$	294	324	*3*

Table S5 Photovoltaic parameters of C_{60}- and PCBM-based perovskite solar cells

ETL	Scan direction	Voc (V)	Jsc (mA cm^{-2})	FF (%)	PCE (%)
C_{60}	Reverse	1.155	24.36	81.41	22.91
	Forward	1.157	24.24	81.03	22.72
PCBM	Reverse	1.132	23.38	79.77	21.12
	Forward	1.13	23.39	79.61	21.05

Table S6 Time-resolved photoluminescence (TRPL) fitting parameters for PVK, PVK/C_{60}/BCP, and PVK/PCBM/BCP films. Time constants were calculated from the TRPL spectra. Lifetime decay components were fitted using a bi-exponential decay model (Fit function = $A_1 e^{-t/\tau_1} + A_2 e^{-t/\tau_2}$).

Sample	A_1 (%)	τ_1 (ns)	A_2 (%)	τ_2 (ns)	τ_{AVG} (ns)
PVK	11.83	50.31	88.17	1632.01	1625.49
PVK/C_{60}/BCP	64.63	49.47	35.37	249.80	196.58
PVK/PCBM/BCP	34.60	63.53	65.40	342.07	317.15

$\tau_{AVG} = (A_1\tau_1^2 + A_2\tau_2^2)/(A_1\tau_1 + A_2\tau_2)$

Table S7 The comparison of the PEC HER performance with the reported perovskite-based photocathode.

Catalyst	J_{ph} @ 0 VRHE (mA cm^{-2})	E_{onset} (V_{RHE})	Electrolyte	H_2 production rate (μmol h^{-1} cm^{-2})*	Ref.
NiCo	–24.00	0.99	1.0 M KOH	447.7	This work
Pt	–22.00	1.06	0.5 M H_2SO_4	410.4	*4*
NiPCoP	–21.98	1.06	1.0 M KOH	410.1	*5*
Pt	–21.70	1.10	0.5 M H_2SO_4	404.8	*6*
NiMo	–21.00	1.03	1.0 M KOH	391.8	*7*
MoS_2	–20.60	1.02	0.5 M H_2SO_4	384.3	*8*
Au–Pt–Ni	–20.13	0.95	0.5 M H_2SO_4	375.5	*9*
Pt	–18.10	0.95	0.5 M H_2SO_4	337.7	*10*
Pt	–14.30	0.95	0.1 M KPi	266.8	*11*
Pt	–12.10	0.60	0.1 M KBi	225.7	*12*
Pt	–9.80	0.95	0.1 M KBi	182.8	*13*
Pt	-10.50	0.68	0.5 M H_2SO_4	195.9	*14*
Pt	-21.00	1.1	0.1 M H_2SO_4	391.8	*15*
Pt	-20.40	1.15	0.5 M H_2SO_4	380.6	*16*

*IF faradaic efficiency=100%, H_2 production rate = $J_{ph}*10^3*3600/(2*96485)$

Table S8 The comparison of the bias-free HER performance with reported PEC cell.

Photocathode	Photoanode	PV	STH	J_{op}^{*} (mA cm^{-2})	Ref.
PVK	-	-	7.62	24.00	This work
CIGS	$BiVO_4$	-	1.01	1.05	*17*
Cu_2O	$BiVO_4$	-	3.00	2.45	*18*
CIGS	$BiVO_4$	-	3.70	3.00	*19*
Sb_2Se_3	$BiVO_4$	-	1.50	1.20	*20*
Si	$BiVO_4$	-	3.50	2.85	*21*
Cu_2O	$BiVO_4$	-	3.24	2.95	*22*
SnS	$BiVO_4$	-	1.70	1.40	*23*
Cu_3BiS_3	$BiVO_4$	-	2.04	1.66	*24*
Si	$BiVO_4$	-	3.70	3.03	*25*
Cu_2ZnSnS_4	$BiVO_4$	-	3.17	2.58	*26*
Si	Sb_2S_3	-	5.24	4.30	*27*
Cu_3BiS_3	$BiVO_4$	-	2.33	1.89	*28*
Si	In_2S_3/CdTe		5.10	4.15	*29*
CIGS	-	PVK	9.04	7.75	*30*
Sb_2Se_3	-	Dual PVK	10.2	8.30	*31*
-	Ta_3N_5	Dual $CuInSe_2$	11.07	9.50	*32*
-	Ta_3N_5	Dual CIS	8.20	6.70	*33*
-	$BiVO_4$	PVK/Si	9.02	7.33	*34*

*Current density of the operating point for PEC cell without external bias.

Reference

1. J. Wang, X. Ma, T. Liu, D. Liu, S. Hao, G. Du, R. Kong, A. M. Asiri, and X. Sun, *Materials Today Energy*, 2017, **3**, 9–14.
2. Z. Pu, I. S. Amiinu, F. Gao, Z. Xu, C. Zhang, W. Li, G. Li, and S. Mu, *Journal of Power Sources*, 2018, **401**, 238–244.
3. R. A. Senthil, S. Jung, A. Min, A. Kumar, C. J. Moon, M. Singh, and M. Y. Choi, *ACS Catalysis*, 2024, **14**, 3320–3335.
4. A. M. Fehr, A. Agrawal, F. Mandani, C. L. Conrad, Q. Jiang, S. Y. Park, O. Alley, B. Li, S. Sidhik, and I. Metcalf, *Nature Communications*, 2023, **14**, 3797.
5. R. Rhee, T. G. Kim, G. Y. Jang, G. Bae, J. H. Lee, S. Lee, S. Kim, S. Jeon, and J. H. Park, *Carbon Energy*, 2023, **5**, e232.
6. J. H. Kim, S. Seo, J. H. Lee, H. Choi, S. Kim, G. Piao, Y. R. Kim, B. Park, J. Lee, and Y. Jung, *Advanced Functional Materials*, 2021, **31**, 2008277.
7. H. Choi, S. Seo, C. J. Yoon, J. B. Ahn, C. S. Kim, Y. Jung, Y. Kim, F. M. Toma, H. Kim, and S. Lee, *Advanced Science*, 2023, **10**, 2303106.
8. H. Choi, S. Seo, J.-H. Kim, J.-H. Lee, S. Kim, G. Piao, H. Park, K. Lee, and S. Lee, 2021.
9. S. Khamgaonkar, Q. Chen, K. Musselman, and V. Maheshwari, *Journal of Materials Chemistry A*, 2023, **11**, 20079–20088.
10. H. Zhang, Z. Yang, W. Yu, H. Wang, W. Ma, X. Zong, and C. Li, *Advanced Energy Materials*, 2018, **8**, 1800795.
11. S. Ahmad, A. Sadhanala, R. L. Hoye, V. Andrei, M. H. Modarres, B. Zhao, J. Ronge, R. Friend, and M. De Volder, *ACS Applied Materials & Interfaces*, 2019, **11**, 23198–23206.
12. V. Andrei, R. L. Hoye, M. Crespo-Quesada, M. Bajada, S. Ahmad, M. De Volder, R. Friend, and E. Reisner, *Advanced Energy Materials*, 2018, **8**, 1801403.
13. M. Crespo-Quesada, L. M. Pazos-Outón, J. Warnan, M. F. Kuehnel, R. H. Friend, and E. Reisner, *Nature Communications*, 2016, **7**, 12555.
14. I. S. Kim, M. J. Pellin, and A. B. Martinson, *ACS Energy Letters*, 2019, **4**, 293–298.
15. J. Park, J. Lee, H. Lee, H. Im, S. Moon, C. S. Jeong, W. Yang, and J. Moon, *Small*, 2023, **19**, 2300174.
16. Y. Choi, R. Mehrotra, S.-H. Lee, T. V. T. Nguyen, I. Lee, J. Kim, H.-Y. Yang, H. Oh, H. Kim, and J.-W. Lee, *Nature Communications*, 2022, **13**, 5709.
17. M. Chen, Y. Liu, C. Li, A. Li, X. Chang, W. Liu, Y. Sun, T. Wang, and J. Gong, *Energy & Environmental Science*, 2018, **11**, 2025–2034.
18. L. Pan, J. H. Kim, M. T. Mayer, M.-K. Son, A. Ummadisingu, J. S. Lee, A. Hagfeldt, J. Luo, and M. Grätzel, *Nature Catalysis*, 2018, **1**, 412–420.
19. H. Kobayashi, N. Sato, M. Orita, Y. Kuang, H. Kaneko, T. Minegishi, T. Yamada, and K. Domen, *Energy & Environmental Science*, 2018, **11**, 3003–3009.
20. W. Yang, J. H. Kim, O. S. Hutter, L. J. Phillips, J. Tan, J. Park, H. Lee, J. D. Major, J. S. Lee, and J. Moon, *Nature Communications*, 2020, **11**, 861.
21. S. Feng, T. Wang, B. Liu, C. Hu, L. Li, Z.-J. Zhao, and J. Gong, *Angewandte Chemie International Edition*, 2020, **59**, 2044–2048.
22. Y. Zhang, H. Lv, Z. Zhang, L. Wang, X. Wu, and H. Xu, *Advanced Materials*, 2021, **33**, 2008264.

23. H. Lee, J. W. Yang, J. Tan, J. Park, S. G. Shim, Y. S. Park, J. Yun, K. Kim, H. W. Jang, and J. Moon, *Advanced Science*, 2021, **8**, 2102458.
24. D. Huang, L. Li, K. Wang, Y. Li, K. Feng, and F. Jiang, *Nature Communications*, 2021, **12**, 3795.
25. B. Liu, S. Wang, S. Feng, H. Li, L. Yang, T. Wang, and J. Gong, *Advanced Functional Materials*, 2021, **31**, 2007222.
26. D. Huang, K. Wang, L. Li, K. Feng, N. An, S. Ikeda, Y. Kuang, Y. Ng, and F. Jiang, *Energy & Environmental Science*, 2021, **14**, 1480–1489.
27. L. Wang, W. Lian, B. Liu, H. Lv, Y. Zhang, X. Wu, T. Wang, J. Gong, T. Chen, and H. Xu, *Advanced Materials*, 2022, **34**, 2200723.
28. S. Moon, J. Park, H. Lee, J. W. Yang, J. Yun, Y. S. Park, J. Lee, H. Im, H. W. Jang, W. Yang, and J. Moon, *Advanced Science*, 2023, **10**, 2206286.
29. Y. Cai, S. Wang, B. Liu, G. Zhang, H. Gao, Y. Tong, Q. Chang, P. Zhang, T. Wang, and J. Gong, *Nature Communications*, 2025, **16**, 5105.
30. B. Koo, D. Kim, P. Boonmongkolras, S. R. Pae, S. Byun, J. Kim, J. H. Lee, D. H. Kim, S. Kim, and B. T. Ahn, *ACS Applied Energy Materials*, 2020, **3**, 2296–2303.
31. W. Yang, J. Park, H.-C. Kwon, O. S. Hutter, L. J. Phillips, J. Tan, H. Lee, J. Lee, S. D. Tilley, and J. D. Major, *Energy & Environmental Science*, 2020, **13**, 4362–4370.
32. Y. Pihosh, V. Nandal, T. Higashi, R. Shoji, R. Bekarevich, H. Nishiyama, T. Yamada, V. Nicolosi, T. Hisatomi, and H. Matsuzaki, *Advanced Energy Materials*, 2023, **13**, 2301327.
33. Y. Kawase, T. Higashi, K. Obata, F. Kishimoto, Y. Pihosh, K. Domen, and K. Takanabe, *Chemistry of Materials*, 2024, **36**, 2390–2401.
34. J. W. Yang, S. G. Ji, C.-S. Jeong, J. Kim, H. R. Kwon, T. H. Lee, S. A. Lee, W. S. Cheon, S. Lee, H. Lee, M. S. Kwon, J. Moon, J. Y. Kim, and H. W. Jang, *Energy & Environmental Science*, 2024, **17**, 2541–2553.